2006 INTERNATIONAL COALBED METHANE SYMPOSIUM

0606

# Capillary Pressure and Wettability Behavior of the Coal-Water-Carbon Dioxide System at High Pressures

W.J. Plug; S. Mazumder; J. Bruining; N. Siemons; K.H. Wolf

Delft University of Technology, Department of Geotechnology

## ABSTRACT

Enhanced Coal Bed Methane (ECBM) combines enhanced recovery of $CH_4$ from coal seams with simultaneous storage of $CO_2$. The efficiency of ECBM depends on the transfer rate between cleats and coal matrix. Diffusive transport of $CO_2$ in the small cleats is enhanced when the coal is $CO_2$-wet. Some coals only become $CO_2$-wet at higher pressures. Indeed for water-wet conditions the small fracture system is filled with water and the rate of $CO_2$ adsorption and $CH_4$ desorption is affected by slow diffusion of $CO_2$.
This paper investigates the wetting behavior of coal, using capillary pressure measurements at in situ conditions. To facilitate the interpretation of these measurements we also obtain capillary pressure curves for an unconsolidated sand sample. We measure both the drainage and imbibition capillary pressure in the coal-water-$CO_2$ system. For medium and high rank coal the primary drainage capillary pressure curves show a water-wet behavior. Secondary imbibition experiments show that the medium rank coal becomes more $CO_2$-wet as the $CO_2$ pressure increases. High rank coal is $CO_2$-wet during primary imbibition. The imbibition behavior is in agreement with contact angle measurements. Hence we conclude that imbibition tests provide the most practically relevant data to evaluate the wetting properties of coal.

## INTRODUCTION

Laboratory studies and recent pilot field tests demonstrate that $CO_2$ injection has the potential to enhance methane production from coal seams. This technology can be employed to sequester large volumes of $CO_2$, thereby reducing emissions of industrial $CO_2$ as a greenhouse gas. The efficiency of $CO_2$ sequestration in coal seams (ECBM), strongly depends on the coal type, the pressure and temperature conditions of the reservoir ([1], [2]) and interfacial interactions (wettability) of the coal-$CO_2$-water system ([3], [4], [5], [6]). It can be expected that in highly fractured coal systems the wetting behavior ([7]) influences the efficiency of ECBM. In the coal-water-$CO_2$ system the preference of the coal surface for the water phase is indicated by the presence of water in the relatively large aggregate of fractures and coal matrix. The main $CO_2$ storage capacity of the coal takes place in the matrix blocks. Depending on the wettability of coal we can distinguish:

1. The coal is water-wet and $CO_2$ and $CH_4$ diffuse in the water filled cleats.
2. The coal is $CO_2$-wet or gas-wet and counter-current capillary diffusion can take place.
3. The coal is gas-wet and binary diffusion of $CO_2$ and $CH_4$ occurs.

Capillary diffusion finds its origin in capillary pressure effects. Capillary pressure ($P_c$) is defined as the pressure difference between the non-wetting and wetting phase and can be seen as a function of surface properties of the coal sample. The storage rate for $CO_2$ is much smaller when the micro cleat system is water-wet. For gas-wet conditions a faster and larger adsorption rate is expected because the diffusion of

$CO_2$ in the gas phase is two to three orders of magnitudes higher than the diffusion of $CO_2$ through water [8].
Dry coal, like dry sand, is naturally hydrophobic and its hydrophobicity varies from one sample to the other due to the wide variation in coalification, genesis and composition of coal [3]. Previous studies, ([3], [4], [5]), were conducted to investigate the hydrophobicity of different coal types. When the rank increases the coal changes from a more amorphous to a more crystalline structure. These micro crystallites are responsible for storage of $CO_2$ and contribute to the capillary pressure properties of the coal. A comparative study of contact angles of air bubbles, oils, flocculants and coagulant drops on flat polished coals surfaces immersed in water was carried out by Orumwens [5]. From these experiments a positive correlation between hydrophobicity and the coal rank of vitrinite rich coals was found. These investigations also concluded that hydrophobicity of coal decreased with decreasing fixed carbon and total carbon content. Another series of experiments carried out by Gutierrrez-Rodriguez et al. ([3], [4]) with air and water on different coal types, varying from high rank to low rank, showed qualitatively the same results. Chi et al. [9] found that the contact angle measured between $CO_2$ and water increased when the pressure varied from atmospheric to 62 bar and more water-wet behavior was found when the ash content of the coal increased. Contact angle measurements with super-critical $CO_2$, using the pendant drop cell, were carried out by Siemons et al. [1 and 2]. These studies concluded that wetting alteration, from water-wet to $CO_2$-wet, for high rank coal occured already at pressures above 2.7 bar and for medium rank coal this alteration was observed for pressure conditions above 85 bar.
Phenomena, like dissolution ([10], [11], [12], [13]), surface tension, gas compressibility and adsorption [14] play an important role during the drainage or imbibition process in coal in the presence of water and $CO_2$ under different pressure and temperature conditions. Chun and Wilkinson [15] investigated the interfacial tension in high pressures $CO_2$–$H_2O$ mixtures. The results showed a mininum for the interfacial tension at the critical pressure (73.8 bar) and temperature (31 ºC).
Adsorption (dissolution) of $CO_2$ on coal changes the physical properties and behavior with respect to hydraulic properties and interfacial interactions. Coal has a highly crosslinked macromolecular network structure and the adsorption of $CO_2$ on coal is associated with a visco-elastic relaxation process. The $CO_2$ will adsorb on the coal and will cause a swelling induced permeability decrease [16]. The higher the pressure the more $CO_2$ can be adsorbed and the more the coal swells [17]. The largest amount of sorption induced swelling in intact coal is about 4 %. It is found that the swelling for grounded coal is much higher than intact coal and has been reported to be in the order of 15 to 20%. The swelling causes a porosity reduction and hence a water saturation increase.
Several methods exist to measure the wettability of rocks, described by Anderson [18]. In this paper we investigate the wettability behavior from the capillary pressure curves obtained for grounded coal at high pressures. Core analysis using capillary pressure curves are extensively discussed over the years by numerous authors. However, as to our knowledge capillary pressure between $CO_2$ and water in coal has not been investigated. Dabbous et al. [19] measured the drainage capillary pressure between air and water of a Pocahontas and Pittsburgh coal at various pressure conditions. They found positive valued capillary pressure curves for both samples. In our work, experimental results for the capillary pressure curves are used to qualify the wetting behavior of coal [20]. The primary imbibition tests provide the most practically relevant data to evaluate the wetting properties of coal. Important in the experiments is the role of temperature and pressure, the rank of coal, swelling effects and the relation between the surface tension and the system pressure. In this paper we define drainage as injection of the gas phase($CO_2$/$N_2$) to displace the water and imbibition as the displacement of gas with water. These definitions are maintained regardless of the wetting conditions of the porous medium considered.

## EXPERIMENTAL SET-UP

The equipment is an optimized version of the set-up presented in Mazumder et al. [20] and is based on the porous plate technique combined with the micro-pore membrane technique, extensively discussed by Jennings et al. [21], Longeron et al. [22] and Christoffersen and Whitson [23]. A schematic diagram of the set-up is shown in Figure 1. The sample holder consists of 3 parts: two end pieces and a stainless steel cylinder with an inner diameter of 84 mm. Two syringe pumps are connected to the in- and outlet of the sample holder and can be set to a constant injection rate (accuracy ± 0.005 ml) or a constant

pressure (accuracy ± 0.1 bar). The gas phase is injected or produced at the top of the sample holder and the water is collected or injected at the bottom using the second syringe pump for pressures > 1 bar. For primary drainage experiments at atmospheric conditions, valve 7 is closed and valve 8 is open and the water is produced in a beaker placed on a mass balance (accuracy ± 0.005 g ). A layer of paraffin on top of the water surface avoids evaporation. Two pressure transducers (GPT and WPT) record the single phase pressures (type, range 0-100 bar, accuracy ± 0.01 bar ) and the differential pressure over the sample is measured by a pressure difference transducer (range 0-500 mbar, accuracy ± 0.1 mbar ). The PDT device measures the pressure difference exactly at the middle of the sample, such that no correction for gravity effects is required.
To maintain a constant temperature a perspex box, sealed by polystyrene, covers the entire set-up. Inside the box two 60 W light-bulbs, which switch on and off, regulate a constant temperature in the range between 25-40 ± 0.5 ºC. As computed from the heat capacity for the sample holder and the sand individually, the characteristic time for the stainless steel is ~400 s and for the sample ~10400 s. Therefore, we allow temperature equilibration for at least two days for gaseous and liquid $CO_2$ / $N_2$ and at least 3 days when supercritical $CO_2$ is used, to ensure the total set up is at equal temperature.
The sample holder, see Figure 2, consists of a stainless steel ring ($H = 2.5$ cm, $D_{sample} = 8.4$ cm), which contains the unconsolidated sample. The grains are kept in place using a combination of plates at the top and bottom of the sample. At the bottom, two porous plates (*Cr-Ni-Steel* basis) with a diameter of, $D_{s,1}$ = 9.0 cm and $D_{s,2}$ = 8.4 cm respectively, a permeability of $2\times10^{-12}$ $m^2$ and a porosity of 0.32, support the sample and protect the hydrophilic membrane used in primary drainage experiments. Two stainless steel plates ($D_{SS,1}$=9.0 cm and $D_{ss,2}$= 8.4 cm ) both with 32 single perforations ($D_p$= 5 mm ) are used at the top directly above the sample in combination with a nylon filter with a pore size of 210 µm. Between the plates a hydrophobic membrane is placed for the primary imbibition process, prohibiting water flow towards the gas production side (Figure 2). To avoid leakage of gas or water over the hydrophobic or hydrophilic membranes we seal the outer perimeter with a rubber O-ring (thickness of 0.21 cm). Concentric flow grooves in the end-pieces redistribute the injected and produced phase over the total sample area to avoid preferential flow and fast breakthrough of the injected phase.

## SAMPLE DESCRIPTION AND PREPARATION

Four types of unconsolidated rock material are used; a fine grained sand, a coarse grained sand, a medium rank coal and a high rank coal. The first series of experiments are conducted on unconsolidated quartz sand using $CO_2$ and $N_2$ as the non-wetting phase. During these reference experiments adsorption of the gas on the solid is assumed to be negligible. The fine grained sand sample has an average grain size of $160<D_{50}<210$ µm and capillary pressure curves are obtained to investigate the reproducibility at atmospheric conditions. The capillary pressure curves obtained for the coarse sand, with $360< D_{50}<410$ µm, are obtained to understand the flow rate dependency of the syringe pump method. Also the system properties were tested for different pressure and temperature conditions.
For the examination of the capillary pressure and wettability behavior in coal we choose two coal samples, used in the work of Siemons et al. ([1], [2]). A medium rank coal Warndt-Luisenthal from Germany and a high rank coal Selar-Cornish from England. The Warndt-Luisenthal coal is high in volatile matter content and low in fixed carbon content compared to the Selar-Cornish sample (see Table 1).The coal samples are collected from a coal matrix, of which 2 kg of coal has been crushed in different grain size fractions. For the coal experiments we use grain size fractions of $500<D_{50}<630$ µm and $250<D_{50}<400$ µm. Properties of the two coal types are presented in Table 1. The moisture content and ash content of the coal samples are determined according the ASTM3173 [23] and ASTM3174 [24] standard method respectively. After each experiment the sample was dried in an oven at a temperature set to 50 ºC.
The reason to use grounded coal samples for the experiments, is to expose this surface area for utmost interaction between the surface, water and $CO_2$. The surface area contained in the void fraction can be significant. Therefore we have measured the surface area. Volumetric physisorption of $CO_2$ at 0 ºC was done to determine the micro pore area and micro pore volume of the void space. This data alongside the composition of the coal samples are reported in Table 1.

## EXPERIMENTAL PROCEDURE

Before the start of each experiment the set-up is cleaned and the porous plates are dried. The assembling of the sample holder is from the bottom upward (see Figure 2). For each experiment we use new millipore filters and new O-rings which are greased with a lubricant. When end piece 2 inclusive the porous plates and O-rings, and the stainless steel ring are mounted together we pour the unconsolidated sample in the sample holder. The sample is vibrated for 10 minutes to obtain a better packing. The last step in assembling the sample holder is to put end piece 1, inclusive the perforated plates, the hydrophobic filter, the nylon filter and O-rings, on top of the stainless steel ring. The sample holder is placed in between valve 4 and 5 and the entire system is evacuated for 1 hour.
The porosity, $\varphi$, is determined with helium at a constant temperature using the ideal gas law with a correction for the compressibility of helium. For the sand and coal samples we found a porosity of 0.36-0.38 and 0.42-0.45 respectively. Subsequently the total system is again evacuated for 1 hour. When an experiment starts with the primary drainage process, the hydrophobic filter is left out. This enables to pressurize the system to dissolve the small air bubbles carried along with the distilled water. In the same way, the hydrophilic filters are removed for primary imbibition tests.
In this paper we consider 3 types of experiments:
*Case 1: Primary drainage at atmospheric pressure, $P=P_{atm}$*
The total sample holder is initially filled with water from valve 5 up to valve 4 (Figure 1). Subsequently the water pump is used to apply a pressure of 10 bar to remove all possible air and to obtain 100% water saturation. We close valve 7 when the required pressure is reached, i.e. the injection rate of water is zero. Due to atmospheric conditions the production side must be connected to the atmosphere and therefore valve 8 is opened and the water pressure decreases towards atmospheric pressure. Because valve 4 is closed no water can flow out the system. The gas tubing and pump are flushed and filled with either $N_2$ or $CO_2$. Finally we set a constant temperature and let the system equilibrate for the time mentioned. The primary drainage experiment starts when a constant gas injection rate is applied and valve 4 is opened. Due to operation restrictions of the syringe pumps for pressures below 1 bar, no secondary imbibition tests are performed for atmospheric conditions.
*Case 2: Primary drainage and secondary imbibition at high pressures, P>1bar*
For this experiment the sample holder is initially filled with water and the water pump is set to the required pressure in order to remove possible air bubbles. Now the system pressure is controlled by the water pump. Valve 4 is closed and the gas tubing and pump are filled with either $N_2$ or $CO_2$. A gas booster, connected to valve 1, is used to bring up the gas pressure to the required value for a specific temperature. We set a constant temperature and let the system equilibrate for the required time. After the system has equilibrated, a constant gas injection rate is applied, the water pump is set to a constant pressure and valve 4 is opened. After the primary drainage process ends, the secondary imbibition process starts when the water pump is set to a constant injection rate and the gas pump is set to a constant production pressure.
*Case 3: Primary imbibition and secondary drainage at high pressures, P>1bar*
The total sample holder is initially filled with gas from valve 5 up to valve 4 (Figure 1) and the water tubing and pump are flushed and filled with water. The same procedure as mentioned previously, is applied to reach the gas pressure for a specific temperature. The absolute pressure is kept constant by the gas pump and the water pressure is increased to the required pressure using the water pump. We set a constant temperature and let the system equilibrate for the desired time. The primary imbibition starts when a constant water injection rate is applied, the gas pump is set to a constant pressure and valve 5 is opened. After the primary drainage process ends, the secondary drainage process starts when the water pump is set to a constant production pressure and the gas pump is set to a constant injection rate.

The water saturation is obtained by the mass of water produced for the atmospheric conditions and by the change in volume of the water pump for high pressure conditions. Moreover the integral mass balance is checked by weighing all the separate parts of the sample holder at the end of the experiment, from which an independent value of the final water saturation in the sample can be found. The mass of water in the sample measured before and after drying the sample has big uncertainties due to depressurizing of the sample holder.
For the high pressure drainage experiments the amount of water in the pump is measured to validate whether only negligible amounts of ‘free’ gas are produced. For imbibition tests we apply essentially the

same procedure to the gas pump to validate that there is only negligible water production. It turns out that the gas volume in the water pump never exceeds one percent of the volume. Water is observed in the gas pump for the secondary imbibition tests conducted on both types of coal samples.
A procedure is developed to analyze the experimental data to obtain the capillary pressure curves based on the following:

- The decrease (increase) in water saturation is computed from the mass produced (injected).
- The initial water (gas-) saturation for primary drainage (imbibition) is 1.
- The viscous pressure drop over the sample holder is negligible (~0.04Pa).
- For the drainage experiments all the water from end-piece 1 and the perforated plates is drained prior to the gas reaches the sample (see Figure 2).
- The beginning of the primary imbibition process is marked by a sudden pressure drop, independent of the water volume injected.
- During the drainage process all the water remains in pore space of the porous plates, hydrophilic filter and the void of end piece 2 (see Figure 2).
- During the primary imbibition process no water is stored in the remaining pore volume of the porous plates.
- Compressibility of water is neglected for all pressure conditions.
- For secondary imbibition we assume that the gas phase has not entered the porous plate.
- The porosity for all samples used is assumed constant during the drainage and imbibition process.

## EXPERIMENTAL RESULTS

We have extensively tested the experimental method for a fine and coarse grained unconsolidated sand samples applying different temperature and pressure conditions using either $N_2$ or $CO_2$ as the non-wetting phase. Moreover, these tests can be used for analysis and comparison with the measurements obtained for the coal samples. More than 19 experiments are conducted for the two types of sand samples and over 15 experiments for two different coal types. A number of tests are duplicates and eight of the experiments are discarded due to system and experimental errors. In this section, we number the experiments in the order of appearance as presented.

### Capillary pressure in unconsolidated sand

The precisionof the method under atmospheric conditions is indicated by the reproducibility of experiments conducted on three different fine sand samples, where a constant $CO_2$ injection rate of 0.5 ml/h is applied (Figure 3). The reproducibility of the experiments based on these results is 2 mbar for the intermediate water satuations ($S_w$ = 0.4-0.85) and around 7 mbar near the end-point saturations.
Calibration of the experimental procedure for continuous gas injection has been investigated for primary drainage. In experiment 4 and 6 (Figure 4) the gas injection rate is altered between 0-1 ml/hr to see the influence on viscous forces and dynamic capillary pressure on the measured $P_c$. No significant effect in capillary pressure is observed for increasing injection rates.
To test the set-up for high pressures and temperatures, drainage and imbibition tests are conducted on the coarse sand sample. A decrease in capillary pressure is measured for increasing $CO_2$ pressures (see Figure 4). Furthermore, a decrease in connate water saturation is observed for increasing system pressures. The capillary pressure measured with liquid $CO_2$ (experiment 6, Figure 4) and super-critical $CO_2$ (experiment 7, Figure 4) are very similar. However, as a result of the phase instabilities of super-critical $CO_2$, small perturbations in the system dynamics cause sudden events, such that water starts to imbibe during the continuous $CO_2$ injection. This results in a decreasing capillary pressure and an irregular drainage curve. The sand sample remains water-wet, indicated by the positive capillary pressure, for all pressure and temperature conditions applied. In Figure 5 the secondary imbibition curves for experiment 5 and 7 are presented. The residual $CO_2$ saturation for the 8 bar pressure condition is around 0.95. For the super-critical conditions (experiment 7) we abort the experiment before the residual gas saturation has reached. From a post-mortem it turns out that no water has been produced in the gas production pump for both experiments 5 and 7. Moreover, a decrease in imbibition capillary pressure is observed for increasing $CO_2$ pressures and the secondary imbibition curves are parallel to each other.

Above $S_w$= 0.5, the capillary pressure becomes negative for super-critical $CO_2$ indicating more $CO_2$-wet behavior.
The injection and production behavior for primary drainage with $CO_2$ under both atmospheric pressure conditions and high pressure conditions (85 bar) is presented in Figure 6. The results for experiment 4 show the solubility and compressibility effects. However, when liquid $CO_2$ is injected (experiment 6) these effects are not observed and the cumulative gas volume injected is equal to the cumulative water volume produced.

In order to improve the analysis of primary imbibition, the wettability and capillary pressure in the porous plates are investigated by two experiments. The first experiment is a continuous water injection from the bottom of the sample holder, in which the oven-dried porous plates were placed. The sample holder remains open and water breakthrough is observed already after 6 ml of water injected. This volume is much smaller than the actual pore volume of 17 ml. The water on top of the filters ( see Figure 7) appears as isolated patches in a hydrophobic environment. The second experiment is a primary imbibition test on coarse sand. We observe again that in the sand the water appears at the top of the sand sample as patches (see Figure 8).

A primary imbibition experiment is conducted for the coarse sand, by water injection in a $N_2$ saturated sand sample (see Figure 5). In Figure 9 the differential pressure and the cumulative water injection is plotted against time for the period prior to the imbibition process. Distinct events can be observed: (A) the differential pressure drops rapidly when the water reaches the porous plates and subsequently (B) it rises towards a stable situation where (C) water is imbibing in the porous plates. The pressure difference increases rapidly at (D) when the sample starts to imbibe the water. The primary imbibition curve is presented in Figure 5. As expected the imbibition capillary pressure curve is positive and the residual gas satuation is 0.16. Because the hydrophobic filter is used no water can be produced in the gas pump. For $S_w$= 0.1-0.4 the data acquisition system has failed and the data are missing.

Capillary pressure in medium and high rank coal

Figure 4 shows the reproducibility for drainage experiments using liquid $CO_2$, in the Warndt-Luisenthal coal (medium rank). The amount of water produced prior to the start of each experiment is in agreement with the volume of the measured cumulative void space in end piece 1, the perforated plates and the nylon filter (see Figure 2). The moment the threshold pressure has reached is similar in all cases (see Figure 10). As can be seen in Figure 11, smooth drainage curves are measured and the connate water saturation of $S_{wc}$=0.1 is similar for all experiments. The positive capillary pressure curves indicate that the medium rank coal is water-wet during the primary drainage process. More detailed information for the drainage capillary pressure is gained when the $CO_2$ injection rate is set to zero (e.g. experiment 11, Figure 11 and 12). During the equilibration $S_w$ remains constant. These equilibration steps are applied for two water saturations, $S_w$ = 0.82 and, $S_w$ = 0.38 (see Figure 12). For both saturations the capillary pressure decreases towards zero. Due to time constraints the equilibrium $P_c$ for $S_w$=0.38 is not fully obtained. The decreasing trend in the decay curve indicates a similar equilibrium $P_c$ as measured for $S_w$ = 0.81.
The results for the secondary imbibition process for the medium rank coal are shown in Figure 13. The amount of water produced in the gas pump indicates an early water breakthrough for all secondary imbibition experiments, except for experiment 15. The post-mortem of the coal samples shows that the water is located at the boundaries of the sample holder. Comparison of the secondary imbibition curves measured in the medium rank coal with sand (e.g., experiment 7, Figure 5) shows that the capillary pressure in coal immediately drops to a negative value, contrary to a gradual decrease of $P_c$ for coarse sand under the same conditions. The pressure dependency of the secondary imbibition capillary pressure is shown in Figure 13. A decrease of the secondary imbibition $P_c$, from positive to negative values, is observed for increasing $CO_2$ pressures. In agreement to Siemons et al. [2] the wettability of the medium rank coal alters for increasing $CO_2$ pressures.
The production and injection data for the primary drainage in medium rank coal (experiment 9) is presented in Figure 14. Similar conditions are applied for experiment 6 (see Figure 6). Comparison

between the water production versus gas injection for experiment 6 and 9, shows that the effect of adsorption is not very pronounced. Similar to the drainage experiment in sand, the cumulative production and injection curves for coal are almost parallel and a small deviation in cumulative volumes is observed. Primary drainage curves obtained for the Selar-Cornish coal (high rank) are shown in Figure 15. A water-wet behavior is observed for all cases. Similar to experiment 7 (Figure 4) the imbibition events (denoted by A,B and C) occur for continuous $CO_2$ injection in the high rank coal.

To understand the mechanism of early water breakthrough during secondary imbibition we perform primary imbibition experiments on the high rank coal. The primary imbibition measurement conducted on sand (Figure 9, experiment 8) is used as reference to indicate the start time of the imbibition process. We use fresh Selar-Cornish samples that have not been exposed to $CO_2$, i.e. no adsorption and swelling has influenced the coal surface. We measure negatively valued capillary pressures, indicating a $CO_2$-wet behavior. Moreover, the behavior in differential pressure prior to the imbibition process does not agree with the data obtained for the primary imbibition for $N_2$ in sand (experiment 8, Figure 9). However, similar behavior for all primary imbibition experiments in high rank coal is found for the filling of the void space of end piece 2. Only 10% of the pore space of the porous plates is saturated. Hence, we can assign the start of the imbibition process. We determine the water saturation after this moment under the assumptions that all the water injected from this moment is present as pore water in the coal sample and the porosity remains constant. Figure 16 shows the primary imbibition curves for the high rank coal using super-critical $CO_2$ (experiment 16,17 and 18) and $CO_2$ in its gaseous state (experiment 19). The $P_c$ measured under the high pressure conditions (>85 bar) is negative, indicating that the high rank coal samples are all $CO_2$-wet. For the situation where $CO_2$ is gaseous (5 bar, experiment 19), we measure positive capillary pressures and a fast water breakthrough. During all the primary imbibition experiments conducted on Selar-Cornish, water breakthrough occurs at intermediate water saturations.

## DISCUSSION

Comparison of the experiments conducted on the coarse sand sample to the coal experiments provides a good understanding of the capillary pressure and wettability behavior of the medium and high rank coal samples. In all cases the sand is water-wet. The irregular behavior of the primary drainage experiment measured for experiment 7 (Figure 4) is ascribed to phase instabilities of the super-critical $CO_2$ due to small system perturbations, like temperature variations (± 0.5 ºC) and corresponding thermal expansion effects causing occasional water imbibition. However, the corresponding secondary imbibition curve is completely smooth (see Figure 5).

For complete water-wet systems the threshold pressure of the $CO_2$-water system is directly related to the surface tension. Indeed in the sand sample the decrease in entry pressure for increasing system pressure can only be partly ascribed to pressure dependence of the surface tension [15]. For the conditions applied in experiment 4 and 6, surface tensions of respectively 71 mN/m and 24 mN/m are reported. The threshold pressures are 14 and 7 mbar for experiment 4 and 6 respectively, which disagrees with the measurement of Chun and Wilkinson [15]. The reason for this behavior is not yet clear to us.

The threshold pressure (7 mbar) measured in experiment 7 is similar with the threshold pressures obtained for the primary drianage experiment conducted on both coal types (Figure 11 and 15). This indicates that $CO_2$-wet conditions for the medium and high rank coal are not observed for the drainage processes. $CO_2$-wet behavior is measured by Siemons et al. [1and 2] for the same coal samples under similar conditions. However, when the system equilibrates by shutting down the injection pump (see experiment 11, Figure 11 and Figure 12), the drainage capillary pressure decreases to more mixed-wet conditions, where $P_c$ approaches zero. A possible explanation is that the surface wetting film is ruptured by the presence of the $CO_2$ [26]. If this is correct, it shows that time scale in laboratory experiments may not be representative for field scale behavior.

The secondary imbibition curves, for the medium rank coal all show negative values, meaning that the coal is $CO_2$-wet (see Figure 13). This conclusion is re-inforced by the fast water breakthrough that occurs for experiment 9 and 10. The $CO_2$-wet behavior of the coal is therefore visible during imbibition. The imbibition experiments are in agreement with the contact angle measurements of Siemons et al. [2], where increasing contact angles were measured for the medium rank coal-water-$CO_2$ system with

increasing pressures. The cross-over from water-wet to $CO_2$-wet behavior occurs at 85 bar [2]. The behavior of the coal experiments is in contrast with the secondary imbibition experiments conducted in coarse sand (experiment 7 and 8). Also in these sand experiments no water breakthrough has been observed, in contrast to the coal experiments. Secondly, from the secondary imbibition process, $CO_2$-wet conditions of the medium rank coal are already visible close to $S_{wc}$. After changing the flow directions the $P_c$ drops immediately to negative values. As opposed to the coal measurements, the secondary imbibition capillary pressure curve of sand (e.g.,experiment 7, Figure 5) shows a gradual decrease in $P_c$ with increasing water saturations.
Negative capillary pressures are also measured for the primary imbibition tests conducted on the high rank Selar-Cornish coal (Figure 16). For super-critical conditions, the coal shows $CO_2$-wet behavior. The fast water breakthrough, also observed for experiment 19 (5 bar, see Figure 16), is indicative of $CO_2$-wet behavior. The results presented in Figure 16 are in agreement with the results obtained by Siemons et al. [1, 2]. For the high rank coal they already found a wetting alteration for system pressures >2.6 bar.
It is our opinion that imbibition experiments provide good qualitative information regarding the wettability of coal.

## CONCLUSIONS

- A capillary pressure set-up that can be used to determine the wettability behavior of the coal-water-$CO_2$ system as a function of the system pressure has been developed.
- The interpretation is facillitated by comparison of the sand-water-$CO_2$ and coal-water-$CO_2$ experiments at a range of pressure and temperature conditions. Reproducibility is considered good.
- Increasing $CO_2$ pressures result in decreasing primary drainage capillary pressures for all samples used. This can only be partly explained by a surface tension change.
- Both the medium and high rank coal are water-wet during the primary drainage process; this behavior is in contrast with contact angle experiments.
- Fast water breakthrough indicates $CO_2$-wet behavior.
- With increasing system pressures the wettability of the medium rank coal alters from water-wet to $CO_2$-wet. High rank coal is $CO_2$-wet during primary imbibition experiments in the entire pressure range. The behavior during imbibition corresponds to contact angle measurement data.
- The difference between imbibition and drainage experiments can be explained by the stability of a water layer on the coal. Such a film must be ruptured before the coal becomes $CO_2$-wet.
- This film rupture may imply that the time scale in laboratory experiments are not representative for field scale behavior.

## ACKNOWLEDGMENTS

The research presented in this paper was carried out as part of the CATO program: $CO_2$ Capture, Transport and Storage in the Netherlands (http://www.co2-cato.nl/). The financial support is gratefully acknowledged. We thank L. Vogt, P.S.A. de Vreede and H.G van Asten for technical support.

## REFERENCES

1. Siemons N., Bruining J., Castelijns H. and K.H. Wolf, 2006: “Pressure Dependence of the Contact Angle in a $CO_2$–$H_2O$–Coal System”, J. Colloid Sci, in press.

2. Siemons N., Bruining J., Wolf K.H. and W.-J. Plug, 2006: ”Pressure Dependence of the $CO_2$ Contact Angle on Bituminous Coal and Semi-Anthracite in Water”, Paper 0605, International Coalbed Methane Symposium, Tusculoosa, Alabama, May 22-26.

3. Gutierrez-Rodriguez J.A., Purcell R.J. and F.F. Aplan, 1984: “Estimating the Hydrophobicity of Coal”, Colloid and surfaces, V. 12, p.1-25.

4. Gutierrez-Rodriguez J.A. and F.F. Aplan, 1984: “The Effect of Oxygen on the Hydrophobicity and Floatability of Coal”, Colloid and surfaces, V. 12, p. 27-51.

5. Orumwense F.F.O., 2001: “Wettability of Coal – a Comparative Study”, Scandinavian Journal of Metallurgy, V. 30, p. 204-211.

6. Keller Jr. D.V., 1987: “The Contact Angle of Water on Coal”, Colloids and surfaces, V. 22 , p. 21-35.

7. Anderson W.G., 1986: “Wettability Literature Survey-Part 1: Rock/Oil /Brine Interactions and the Effects of Core Handling on Wettability”, JPT, N. 13932, p. 1125 – 1144.

8. Bird R.B., Steward W.E. and E.N. Lightfoot, 1960: Transport Phenomena: New York, John Wiley & Sons, 780 p.

9. Chi S.-M., Morsi B.I., Klinzing G.E. and S.-H. Chiang, 1987: “Study of Interfacial Properties in the Liquid $CO_2$–Water–Coal System”, Energy & Fuels, V. 2, p. 141-145.

10. Chapoy A., Mohammadi A.H., Chareton A., Tohidi B. and D. Richon, 2004: “Measurement and Modeling of Gas Solubility and Literature Review of the Properties for the Carbon Dioxide-Water System”, Ind. Eng. Chem. Res., V. 43, p. 1794-1802.

11. Diamond L.W. and N.N. Akinfiev, 2003: “Solubility of CO2 in Water from -1.5 to 100 $^oC$ and from 0.1 to 100 MPa: Evaluation of Literature Data and Thermodynamic Modeling”, Fluid Phase Equilibria, V. 208, p. 265—290.

12. Caroll J.J., Slupsky J.D. and A.E. Mather, 1991: “The Solubility of Carbon Dioxide in Water at Low Pressure”, J. Phy. Chem. Ref. Data, V. 20, Nr. 6.

13. Wiebe R. and V.L. Gaddy, 1940: “The Solubility of Carbon Dioxide in Water at Various Temperatures from 12 to 40$^o$ and at Pressures to 500 Atmospheres. Critical Phenomena”, J. Am. Chem. Soc., V. 62, p. 815-817.

14. Siemons N., Busch A., Bruining J. and B. Krooss, 2003: “Assessing the Kinetics and Capacity of Adsorption in Coals by a Combined Adsorption/Diffusion method”, paper SPE 84340, Proceedings of the SPE Annual Technical Conference and Exhibition, Denver, Colorado.

15. Chun B.S. and G.T. Wilkinson, 1995: “Interfacial Tension in High-pressure Carbon Dioxide Mixtures”, Ind. Eng. Chem. Res., V. 34, p. 4371-4377.

16. Mazumder S., Karnik A., and K-H.A.A Wolf., 2006: “Swelling of Coal in Response to CO2 Sequestration for ECBM and its Effect on Fracture Permeability”, In Press for SPE Journal, SPE-97754-RMS.

17. Reucroft P.J. and A.R. Sethuraman, 1987: “Effect of Pressure on Carbon Dioxide Induced Coal Swelling”, Energy & Fuels, V.1, p72-75.

18. Anderson W.G., 1986: “Wettability Literature Survey-Part 2: Wettability Measurement”, JPT, SPE 13933, p. 1246-1262.

19. Dabbous M.K., Reznik A.A., Mody B.G., Fulton P.F. and J. J. Taber, 1975: “Gas-Water Capillary Pressure in Coal at Various Overburden Pressures”, paper SPE 5348, Proceedings of the SPE-AIME Rocky Mountain Regional Meeting, Denver, Colorado.

20. Mazumder S., Plug W.J., and J. Bruining, 2003: “Capillary Pressure and Wettability Behavior of Coal–Water–Carbon Dioxide System”, paper SPE 84339, Proceedings of the SPE Annual Technical Conference and Exhibition, Denver, Colorado.

21. Jennings Jr. J.W, McGregor D.S. and R.A. Morse, 1988: “Simultaneous Pressure and by Automatic Determination of Capillary Relative Permeability History Matching”, SPE Formation Evaluation, SPE 14418, p. 322 – 328.

22. Longeron D., Hammervold W. L. and S. M. Skjaeveland, 1995: ”Water-Oil Capillary Pressure and Wettability Measurements Using Micropore Membrane Technique”, paper SPE 30006, Proceedings of the International Meeting on Petroleum Engineering, Beijing.

23. Christoffersen K.R. and C.H. Whitson, 1995: “Gas/Oil Capillary Pressure of Chalk at Elevated Pressures”, SPE Formation Evaluation, SPE 26613, p 153-159.

24. Standard Test Method for Moisture in the Analysis Sample of Coal and Coke, ASTM D3173.

25. Standard Test Method for Ash in the Analysis Sample of Coal and Coke from Coal, ASTM D3174.

26. Hirasaki G.J., 1991: ”Wettability: Fundamentals and Surface Forces”, SPE Formation Evaluation, SPE 17367, p 217-232.

## TABLES

**Table 1 Coal properties of the medium rank and high rank coal**

| | ***Warndt-Luisenthal*** | ***Selar-Cornish*** |
|---|---|---|
| ***Location*** | Saarbruecken, Germany | Selar, South Wales, UK |
| ***Stratigraphy*** | Westphalian C | Westphalian B |
| ***Proximate analysis*** | | |
| *rank* | hvBb | Semi-anthracite |
| *moisture [%]* | 1.39 | 1.26 |
| *Volatile matter (w.f.) [%]* | 40.51 | 10.35 |
| *Ash (w.f.) [%]* | 2.77 | 3.94 |
| *Fixed Carbon (d.a.f.) [%]* | 58.36 | 89.27 |
| ***Ultimate analysis*** | | |
| *Carbon [%]* | 81.3 | 85.68 |
| *Hydrogen [%]* | 5.58 | 3.36 |
| *Nitrogen [%]* | 1.88 | 1.56 |
| *Sulphur [%]* | 0.69 | 0.68 |
| *Oxygen (diff.) [%]* | 5.47 | 5.58 |
| *H/C* | 0.82 | 0.47 |
| *O/C* | 0.05 | 0.05 |
| ***Coal Petrology*** | | |
| $V_{max}$ *[%]* | 0.71 | 2.41 |
| *Vitrinite* | 74.4 | 73.6 |
| *Liptinite* | 15.6 | 0 |
| *Inertinite* | 9 | 24.6 |
| *Minerals* | 1 | 1.8 |
| ***Internal properties*** | | |
| *Specific surface [$m^2/g$]* | 104 | 208 |
| *Micropore volume [$cm^3/g$] coal* | 0.03545 | 0.071 |

## FIGURES

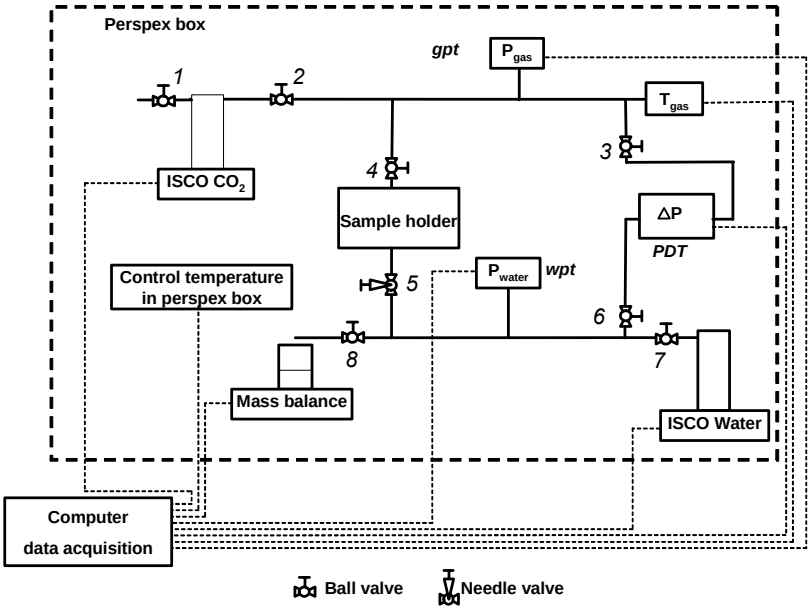


**Figure 1 Schematic lay-out of experimental set-up**

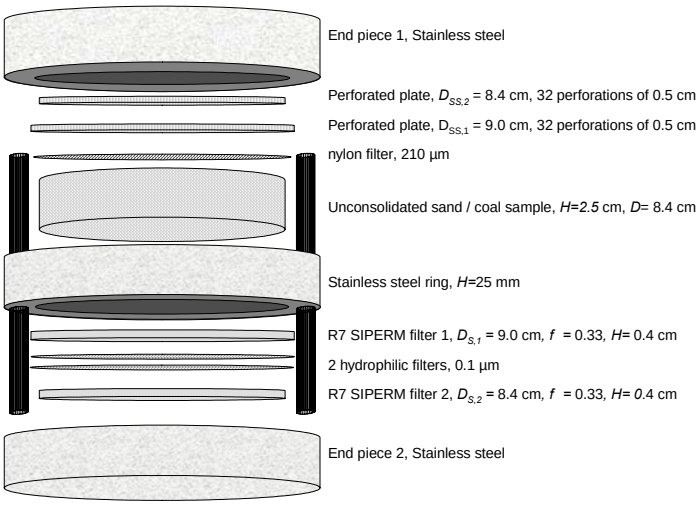


**Figure 2 Sample holder configuration**

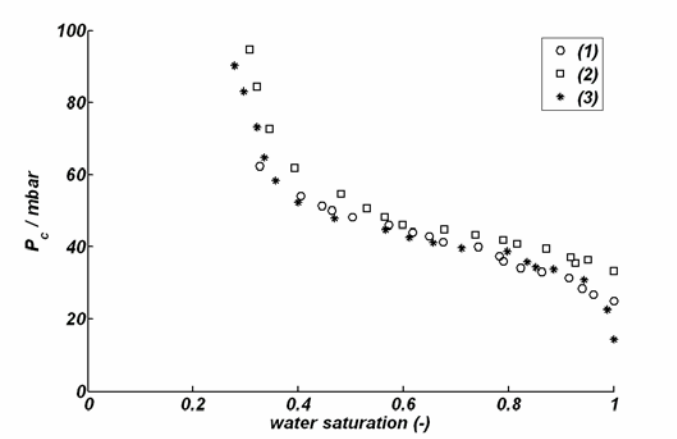


**Figure 3 Primary drainage curves for $CO_2$ in fine sand obtained under atmospheric conditions**

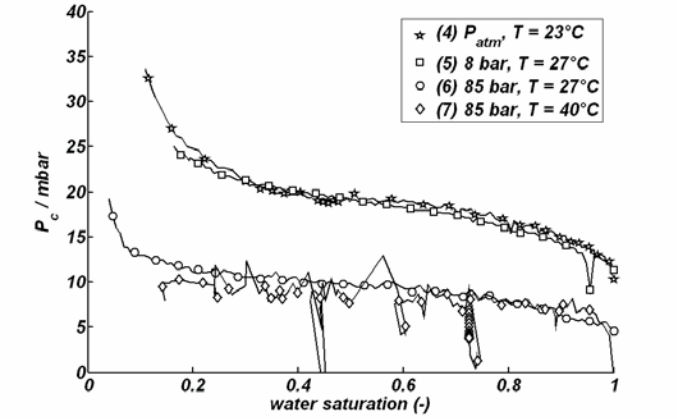


**Figure 4 Primary drainage curves for $CO_2$ injection (0.5 ml/hr) in coarse sand at various pressure and temperature conditions**

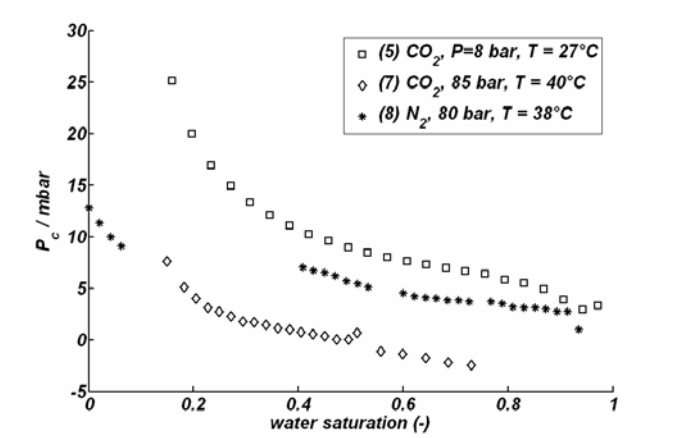


**Figure 5 Imbibition experiments (water injection rate is 0.5 ml/hr) in coarse sand for $N_2$ and $CO_2$ at various pressure and temperature conditions, where the primary imbibition curve is obtained for experiment 8**

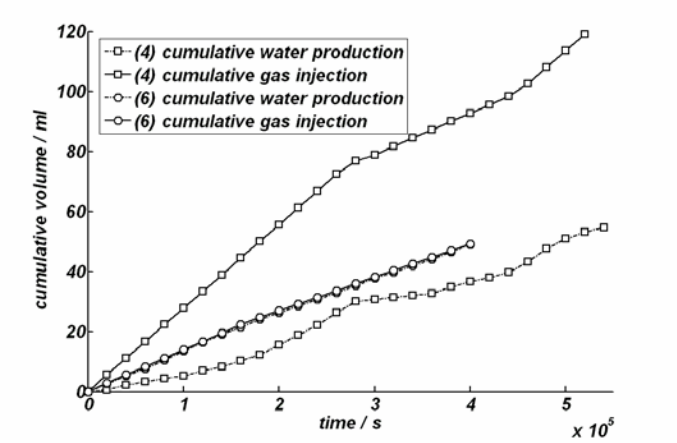


**Figure 6 Cumulative water production and gas injection for drainage with gaseous $CO_2$ (4) and liquid $CO_2$ (6) in coarse sand**

**Figure 7 Water breakthrough in the porous plates: hydrophilic patches embedded in a hydrophobic environment**

**Figure 8 Visualization experiment: water breakthrough in a coarse sand sample**

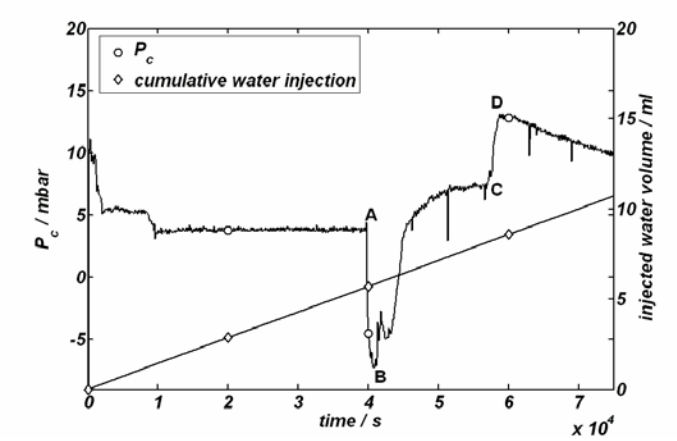


**Figure 9 Evolution of differential pressure for a primary imbibition process (experiment 37, water injection rate is 0.5 ml/hr)**

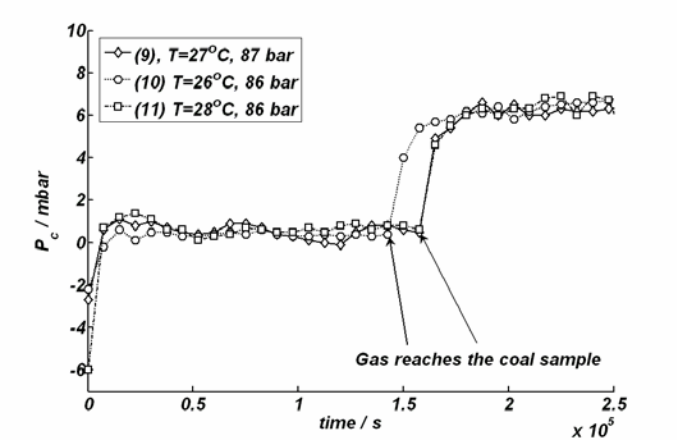


**Figure 10 Evolution of differential pressure for primary drainage ($CO_2$ injection rate is 0.5 ml/hr)**

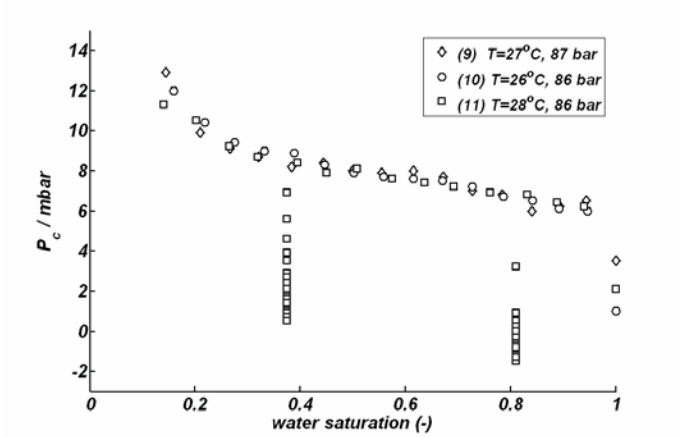


**Figure 11 Primary drainage for $CO_2$ injection (0.5 ml/hr) in Warndt-Luisenthal coal**

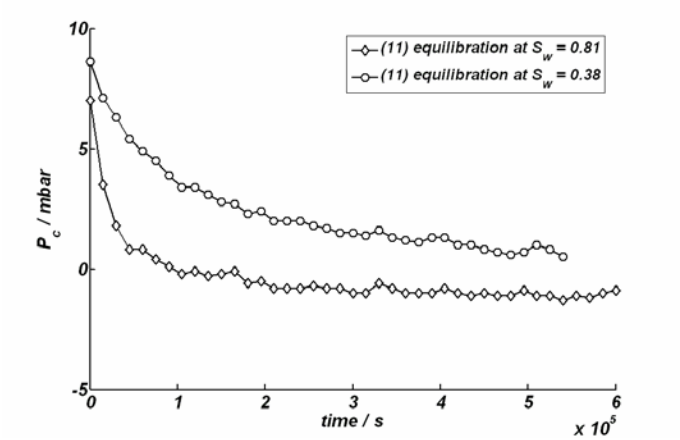


**Figure 12 Equilibriation of $P_c$ for experiment 11 at two different water saturations**

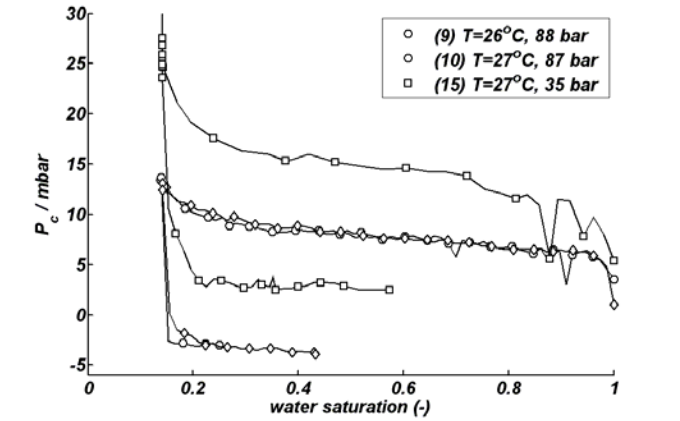


**Figure 13 Primary drainage and secondary imbibition in Warndt-Luisenthal coal (water injection rate is 0.5 ml/hr)**

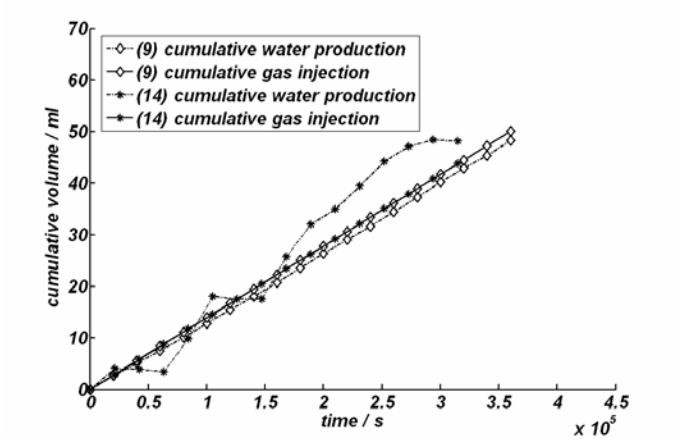


**Figure 14 Cumulative water production and gas injection for drainage with liquid $CO_2$ in medium rank coal (9) and super-critical $CO_2$ in high rank coal (14)**

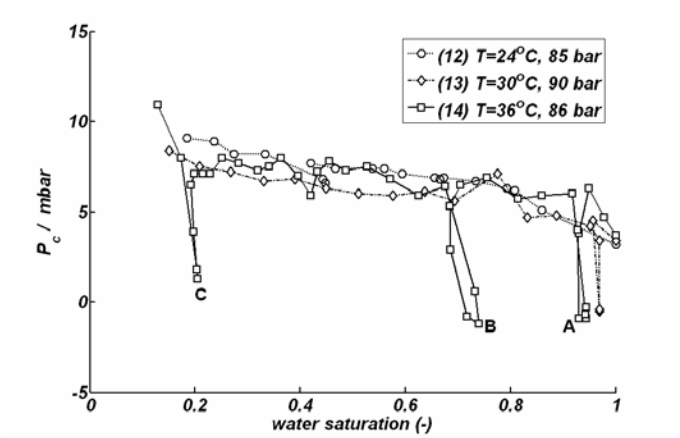


**Figure 15 Primary drainage for $CO_2$ injection (0.5 ml/hr) in high rank Selar-Cornish coal**

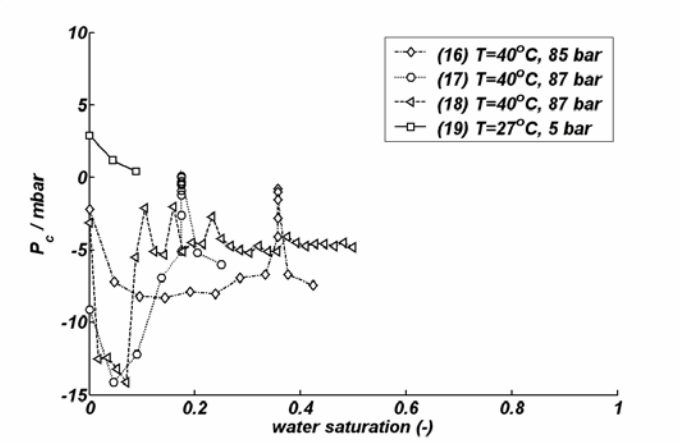


**Figure 16 Primary imbibition in Selar-Cornish at for super-critical and gaseous $CO_2$ (water injection rate is 0.5 ml/hr)**